

Using quantum interferometers to make measurements at the Heisenberg limit

J. DUNNINGHAM*† and T. KIM‡

†School of Physics and Astronomy, University of Leeds,
 Leeds LS2 9JT, UK

‡Department of Physics, University of Ulsan, Ulsan 680-749, Korea

(Received 23 August 2005)

In recent work we proposed a quantum interferometer and showed how it could be used to significantly enhance the resolution that could be achieved in measurement schemes. In this paper, we outline a detailed scheme on how these quantum interferometers could be implemented. We also analyze the effects of dissipation and of imperfect detectors and show that this scheme is remarkably robust to both. This suggests that quantum interferometers may provide a promising route for implementing sub-shot-noise limited measurements in the laboratory.

1. Introduction

A major factor in the advancement of science has been the ability to test new theories with increasingly precise measurements of physical systems. Considerable theoretical and experimental efforts have therefore been devoted to making ongoing improvements in metrology. One of the key developments in the field was the interferometer, which enabled path length differences to be detected through phase shifts with unprecedented accuracy. In particular, it allowed phases to be measured to the ‘shot noise limit’, where the uncertainty scales as $1/\sqrt{N}$ and N is the total number of particles involved. The discovery of non-classical (e.g. squeezed) states of light [1–5] further enhanced the precision that could be achieved. By using squeezed light with reduced phase fluctuations as the input to an interferometer [6], it is possible to detect phase shifts below the shot noise limit and even approach the Heisenberg limit where the uncertainty scales as $1/N$ [7]. This favourable scaling with N means that, for large numbers of particles, a dramatic improvement in measurement resolution should be possible. This may be of great importance in a number of areas of physics including, for example, the detection of gravitational waves.

*Corresponding author. Email: j.dunningham@physics.ox.ac.uk

One possibility for reaching the Heisenberg limit is to use dual Fock states as the input to an interferometer, i.e. when each input port of the interferometer has precisely the same number of particles [8]. This proposal has spawned a great deal of interest particularly with regard to the details of its implementation. Kim *et al.* showed that the number correlated light from an optical parametric oscillator (OPO) or amplifier (OPA) would be a practical alternative to the dual Fock state input [9] and recent experiments have demonstrated Heisenberg-limited interferometry with ultrastable twin beams [10].

One problem with these schemes, however, is that the phase information cannot be determined simply by measuring the population imbalance at the output ports, as is the case for standard interferometry. Instead we need to measure coincidences or correlations between the particles [9]. Such measurements have been shown to be extremely sensitive to any imperfections in the detectors, which suggests that these schemes are likely to be impractical [11]. One possibility is to use Bayes' theorem to analyze the information that can be gleaned from the detections [8, 12]. Other promising proposals as to how this problem can be overcome include disentangling the particles before measurements are made on them [13] or measuring the collapses and revivals of the visibility of interference fringes for Bose-Einstein condensates [14].

In recent work [15], we demonstrated a different route to achieving sub-shot-noise limited measurements. This involved using 'quantum beam splitters' to create maximally entangled states inside the interferometer. In the present paper, we provide more detail on how this scheme could be implemented and show that it has the highly favourable properties of being robust to the effects of both dissipation and imperfect detectors.

We begin in section 2 by illustrating the usefulness of entanglement in precision measurements. We calculate the resolution that can be achieved with a stream of independent particles in an interferometer and compare this with the result for entangled particles. We show that, although entanglement enables a significant improvement, it comes at the price of placing severe restrictions on the detector efficiencies that can be tolerated. In section 3 we outline a scheme for implementing quantum beam splitters and, in section 4, we show how these can be combined to create a quantum interferometer. An analysis of the quantum interferometer shows that it enables measurements to be made below the shot noise limit and circumvents the problems associated with detector efficiencies that have derailed other schemes. Finally in section 5, we discuss the effects of loss and show that this too does not prevent us from approaching the Heisenberg limit. Their robustness to these imperfections suggests that quantum interferometers are promising candidates for implementing sub-shot-noise measurement schemes in the laboratory.

2. Why is entanglement useful for measurements?

In this section, we want to illustrate how entanglement can improve the precision of measurements. We consider the case of a Mach-Zehnder interferometer which consists of two 50:50 beam splitters and a phase shift, ϕ , on one of the

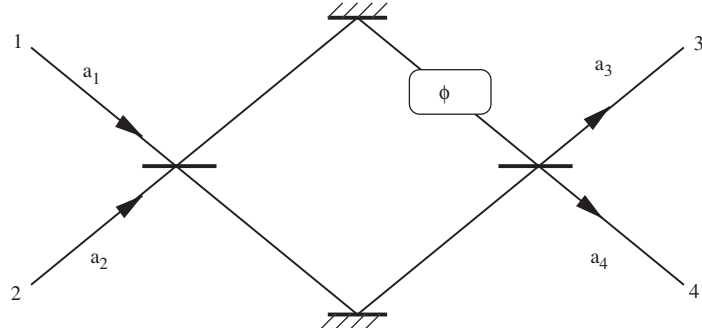


Figure 1. Schematic of a standard Mach-Zehnder interferometer consisting of two mirrors, two 50:50 beam splitters, and a phase shift, ϕ .

paths (see figure 1). Each beam splitter transforms the annihilation operators, a_1 and a_2 at the inputs according to

$$\begin{pmatrix} a_1 \\ a_2 \end{pmatrix} \rightarrow \frac{1}{\sqrt{2}} \begin{pmatrix} 1 & i \\ i & 1 \end{pmatrix} \begin{pmatrix} a_1 \\ a_2 \end{pmatrix}. \quad (1)$$

The total transformation of the operators by the interferometer is therefore,

$$\begin{aligned} \begin{pmatrix} a_1 \\ a_2 \end{pmatrix} &= \frac{1}{2} \begin{pmatrix} 1 & i \\ i & 1 \end{pmatrix} \begin{pmatrix} e^{i\phi} & 0 \\ 0 & 1 \end{pmatrix} \begin{pmatrix} 1 & i \\ i & 1 \end{pmatrix} \begin{pmatrix} a_3 \\ a_4 \end{pmatrix} \\ &= \begin{pmatrix} \sin(\phi/2) & \cos(\phi/2) \\ \cos(\phi/2) & -\sin(\phi/2) \end{pmatrix} \begin{pmatrix} a_3 \\ a_4 \end{pmatrix}, \end{aligned} \quad (2)$$

where a_3 and a_4 are the annihilation operators at the outputs (see figure 1) and we have neglected an unimportant overall phase in the last line. If a particle enters the interferometer at port 1, i.e. the input state is $|1, 0\rangle = a_1^\dagger |0, 0\rangle$, it is clear from (2) that the output state is, $|\psi\rangle = \sin(\phi/2)|1, 0\rangle + \cos(\phi/2)|0, 1\rangle$ and the probabilities that the particle emerges in ports 3 and 4 are,

$$P_3 = \sin^2(\phi/2) \quad (3)$$

$$P_4 = \cos^2(\phi/2). \quad (4)$$

We can treat a stream of N particles independently if they do not interact with one another. This means that the number of particles at the two output ports is given by a binomial distribution. The joint probability that m and $N-m$ particles are detected at ports 3 and 4 respectively is then,

$$P(m, N-m) = \binom{N}{m} P_3^m P_4^{N-m} = \binom{N}{m} \cos^{2m}(\phi/2) \sin^{2(N-m)}(\phi/2), \quad (5)$$

and the mean number of particles detected at port 3 is $\langle n_3 \rangle = N \cos^2(\phi/2)$. So, by measuring the populations at the outputs, we can infer the phase shift, ϕ . This is the principle behind interferometric measurements. Furthermore, we can

estimate the uncertainty in our measurement of ϕ from the variance in the number of particles detected at each port,

$$(\Delta n_3)^2 = (\Delta n_4)^2 = NP_3P_4 = N \sin^2(\phi/2) \cos^2(\phi/2). \quad (6)$$

This uncertainty in particle number can be converted into an uncertainty in the phase shift by a straightforward manipulation of the errors,

$$(\Delta n_3)^2 = \left(\frac{\partial \langle n_3 \rangle}{\partial \phi} \right)^2 (\Delta \phi)^2. \quad (7)$$

Rearranging and substituting for $\langle n_3 \rangle$ and $(\Delta n_3)^2$, we obtain,

$$(\Delta \phi)^2 = \frac{1}{N}. \quad (8)$$

This means that the precision, $\Delta \phi$, with which we can measure the phase shift in the interferometer scales as $1/\sqrt{N}$. This is the so-called shot noise limit and is a consequence of assuming independent particle statistics. By inputting increasingly large numbers of particles, it is possible to improve the measurement resolution to the level required. This approach to interferometry has been highly successful and is used in a wide range of contexts.

We would now like to consider what happens if we remove the assumption that each of the particles can be treated independently. In particular, we would like to see whether it is possible to improve the measurement resolution that can be achieved with the same resources, i.e. the same number of particles. We shall consider the specific case of ‘NOON’ states [16] of the form,

$$|\psi\rangle = \frac{1}{\sqrt{2}} (|N, 0\rangle + e^{i\xi}|0, N\rangle), \quad (9)$$

where $|k, l\rangle$ represents the number of particles on each of the two paths and ξ is a phase between the two terms. The NOON state is a macroscopic superposition of all the particles being on one path of the interferometer and all on the other. Bollinger *et al.* first proposed the idea of using such maximally entangled states to make precise measurements of the frequency of atomic transitions [17]. They showed that the resolution that could be achieved by this technique scales inversely with the total number of particles, $\Delta \phi \sim 1/N$.

NOON states can be created inside an interferometer by replacing the first beam splitter with a ‘quantum beam splitter’ and in section 3 we will discuss a specific scheme for realizing such a device. The particles in the NOON state are entangled since, unlike the previous case, we cannot write the total state of the system as a product of the states of each individual particle.

After a phase shift, ϕ on one arm of the interferometer, the NOON state becomes, $|\psi\rangle = (e^{iN\phi}|N, 0\rangle + e^{i\xi}|0, N\rangle)/\sqrt{2}$. This can be written as,

$$|\psi\rangle = \frac{1}{\sqrt{N!2}} \left[\left(e^{i\phi} a_1^\dagger \right)^N + e^{i\xi} \left(a_2^\dagger \right)^N \right] |0, 0\rangle. \quad (10)$$

If we now pass this state through the second (ordinary) beam splitter of figure 1, the output can be found by transforming each of the operators according to (1). This gives,

$$|\psi\rangle = \frac{1}{\sqrt{2^{N-1}}} \sum_{m=0}^N \binom{N}{m}^{1/2} \cos\left\{\frac{1}{2}[N\phi - \zeta + \pi(m - N/2)]\right\} |m, N-m\rangle. \quad (11)$$

If we were to detect m and $N-m$ particles at ports 3 and 4 respectively, the conditional probability distribution describing our knowledge of ϕ is given by Bayes' theorem, $P(\phi|m, N-m) \propto P(m, N-m|\phi)P(\phi)$. If we have no prior knowledge of ϕ , we take $P(\phi)$ to be flat. This gives,

$$P(\phi|m, N-m) \propto |\langle m, N-m|\psi\rangle|^2 \propto 1 + (-1)^m \cos[N(\phi - \pi/2) - \zeta]. \quad (12)$$

We see that the fringes vary N times faster with ϕ in this case than they do for independent particles. This means that ϕ should be measurable with a resolution that scales as $1/N$ as compared with $1/\sqrt{N}$ for independent particles and demonstrates why entanglement may be useful in precision measurement schemes.

However, along with this enhanced resolution comes a problem. We see from (12) that by changing the value of m by one, i.e. $\Delta m = \pm 1$, the fringes are exactly out of phase with what they were before. This means that if the number of particles that emerge from each port is not measured exactly, the interference fringes wash out and we do not obtain any information about ϕ . Similar results have been expressed elsewhere in terms of the parity of the detected particles [18] (i.e. whether an odd or even number are detected), correlations between the detected particles [15], and which-path information in the system [19].

The fact that every particle must be detected imposes prohibitively strict conditions on the required detector efficiencies and threatens to consign this scheme to being little more than a theoretical curiosity. It turns out, however, that it is possible to overcome this major problem. We shall discuss how this can be achieved in section 4 but, before we do that, it is worthwhile considering a detailed scheme as to how NOON states may be created.

3. Scheme for a quantum beam splitter

We shall use the general term ‘quantum beam splitter’ to refer to any scheme or device that creates a NOON state of the form of (9) from the initial state $|\psi\rangle = |N, 0\rangle$. A quantum beam splitter is quite distinct from an ordinary beam splitter, which, for the same input, would give a binomial distribution of particles at the outputs. The operation of a quantum beam splitter can be seen to be equivalent to that of an ordinary beam splitter if all the particles were somehow ‘stuck together’.

Various proposals have been made for producing NOON states in the laboratory. These include the use of Fredkin gates [20–22], quantum switching [23], coupling a quantum superposition state to a beam splitter [24], and coupling the spin states and collective motion of trapped ions [25]. Experiments have successfully

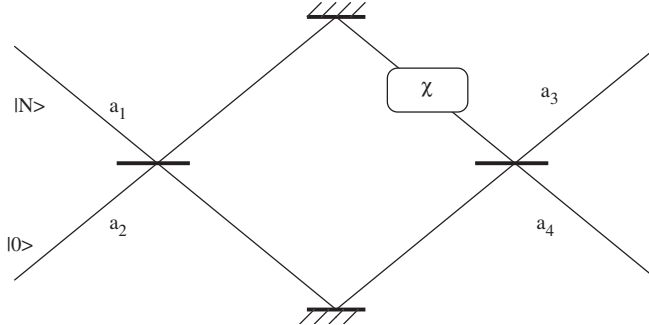


Figure 2. Schematic of a quantum beam splitter. This consists of an ordinary Mach-Zehnder interferometer but with a nonlinearity, χ , on one arm.

created NOON states with three photons [26], and four ${}^9\text{Be}^+$ ions [27], and could in principle be scaled up to larger numbers. A particularly promising theoretical scheme involves making use of ordinary beam splitters and nonlinear unitary evolution to produce states of the form of (9) [28]. This scheme is shown in figure 2 and consists of a standard Mach-Zehnder interferometer with a phase shift on one arm that depends quadratically on the number of particles in that arm. We can study this device by explicitly calculating the transformation it performs on the input state $|\psi\rangle = |N, 0\rangle$.

The unitary operator for a 50:50 beam splitter is,

$$U = \exp\left[-i\frac{\pi}{4}(a_1^\dagger a_2 + a_2^\dagger a_1)\right], \quad (13)$$

where, as before, a_1 and a_2 are the annihilation operators for particles in each of the two input ports. If we consider successive operations of (13) on the initial state, the outputs we obtain are,

$$|N, 0\rangle \rightarrow |\psi_1\rangle \rightarrow (-i)^N |0, N\rangle \rightarrow (-1)^N |\psi_1\rangle^* \rightarrow (-1)^N |N, 0\rangle, \quad (14)$$

where

$$|\psi_1\rangle = \frac{1}{\sqrt{2^N}} \sum_{k=0}^N \binom{N}{k}^{1/2} e^{-i\pi(N-k)/2} |k, N-k\rangle, \quad (15)$$

and $|\psi_1\rangle^*$ is the complex conjugate of $|\psi_1\rangle$. The operation of a balanced beam splitter is cyclic: four successive operations of (13) return the system to its original state, apart from an overall phase.

We can use (14) to understand the action of the scheme depicted in figure 2. If we begin with the state $|\psi\rangle = |N, 0\rangle$ and pass it through the first beam splitter, it is transformed to $|\psi_1\rangle$. The operator corresponding to the nonlinear evolution has the form $\exp(-i\chi t(a_1^\dagger a_1)^2)$, where χ is a parameter governing the strength of the nonlinearity and t is the duration of the nonlinear evolution. This operation could be implemented with nonlinear crystals for photons or by exploiting the

interactions between atoms in Bose-Einstein condensates. If we choose $\chi t = \pi/2$, after this transformation, the state becomes,

$$e^{-i\pi(a_1^\dagger a_1)^2/2} |\psi_1\rangle = \frac{(-i)^N}{\sqrt{2^N}} \sum_{k=0}^N \binom{N}{k}^{1/2} e^{-i\pi k(k-1)/2} |k, N-k\rangle. \quad (16)$$

It is straightforward to check that, since k can only take integer values, this can be written equivalently as,

$$|\psi\rangle = \frac{(-i)^N}{\sqrt{2^{N+1}}} e^{-i\pi/4} \sum_{k=0}^N \binom{N}{k}^{1/2} (e^{i\pi k/2} + ie^{-i\pi k/2}) |k, N-k\rangle \quad (17)$$

$$= \frac{1}{\sqrt{2}} e^{-i\pi/4} [|\psi_1\rangle + i(-1)^N |\psi_1\rangle^*]. \quad (18)$$

Finally, we pass this state through the second beam splitter. We can see from (14) how each term is transformed. The total transformation of the interferometer depicted in figure 2 is therefore

$$|N, 0\rangle \longrightarrow \frac{(-1)^N}{\sqrt{2}} e^{i\pi/4} (|N, 0\rangle + i^{N-1} |0, N\rangle). \quad (19)$$

Ignoring the irrelevant overall phase, we see that the interferometer creates a state of the general form of (9) where $\zeta = \pi(N-1)/2$. A similar calculation for the converse input state reveals,

$$|0, N\rangle \longrightarrow \frac{1}{\sqrt{2}} e^{i\pi/4} [|0, N\rangle + (-1)^N i^{N-1} |N, 0\rangle]. \quad (20)$$

This shows how a simple scheme combining a Mach-Zehnder interferometer with nonlinear evolution allows us to create NOON states of the form we want for precision measurements. Furthermore, we shall show in section 5 that this scheme is not completely destroyed by loss and that we do not need to create perfect NOON states to realise much of the associated advantage in interferometry. This suggests that this scheme may be feasible in future experiments.

Of course, if we were to use these NOON states directly in measurement schemes as discussed above, we would run into difficulties associated with detector efficiencies. We now discuss how this major problem can be circumvented by combining quantum beam splitters to create a ‘quantum interferometer’.

4. The quantum interferometer

A quantum interferometer is simply a Mach-Zehnder interferometer where both beam splitters have been replaced with quantum beam splitters. This set-up is shown in figure 3. Since, as discussed above, a quantum beam splitter can be realised with a nonlinear Mach-Zehnder interferometer, a quantum interferometer can equivalently be depicted schematically by figure 4. In this set-up, the nonlinearities are placed on

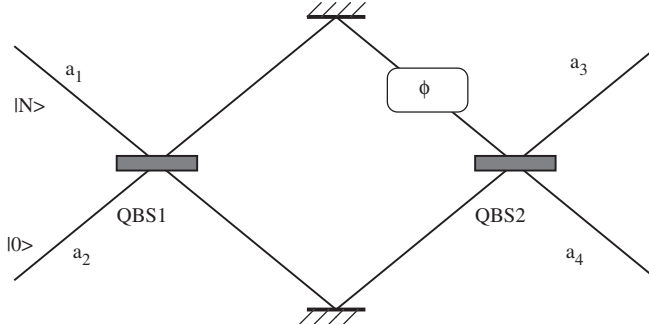


Figure 3. Schematic of a Mach-Zehnder quantum interferometer composed of two quantum beam splitters.

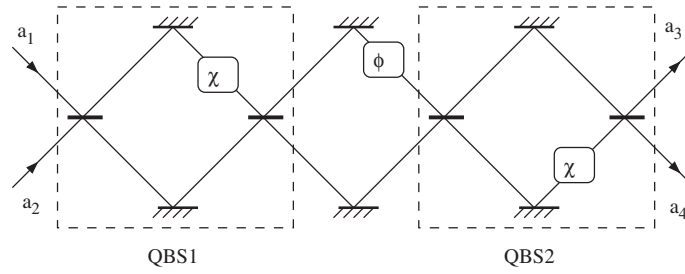


Figure 4. Full scheme for a Mach-Zehnder quantum interferometer. Each of the quantum beam splitters in figure 3 has been replaced with a Mach-Zehnder interferometer with a nonlinearity on one path.

different arms of the two quantum beam splitters to ensure the correct phases are obtained.

We would now like to consider the output from this quantum interferometer and demonstrate that measurement schemes which make use of this technique are not undermined by the effects of detector inefficiencies. If we start with the input state $|\psi\rangle = |N, 0\rangle$ then, after the first quantum beam splitter (QBS1), the state is given by (19). If there is a phase shift, ϕ on one arm as shown in figure 3, the state becomes,

$$|\psi\rangle = \frac{(-1)^N}{\sqrt{2}} e^{i\pi/4} (e^{iN\phi} |N, 0\rangle + i^{N-1} |0, N\rangle). \quad (21)$$

Finally, we pass this state through a second quantum beam splitter (QBS2). It is straightforward to see how (21) is transformed by this operation by using (19) and (20). This gives as the output state,

$$|\psi\rangle = \frac{i}{2} [(-1)^N (e^{iN\phi} - 1) |N, 0\rangle + i^{N-1} (e^{iN\phi} + 1) |0, N\rangle]. \quad (22)$$

We can see from the form of this state that all N particles will be detected at one output or all N at the other. This suggests that this scheme will be robust against the

effects of imperfect detectors since, even if some of the particles are not detected, we still know with certainty at which port they all emerged. The probabilities of detecting all the particles at output ports 3 and 4 respectively are given by,

$$P_3 = \sin^2(N\phi/2) \quad (23)$$

$$P_4 = \cos^2(N\phi/2). \quad (24)$$

Comparing this result with (3) and (4) we see that there is an N -fold enhancement in the phase shift relative to the result for standard interferometry.

Following the standard approach to interferometry, we take the population difference between the outputs as our signal, i.e. $n = a_4^\dagger a_4 - a_3^\dagger a_3 = N - 2a_3^\dagger a_3$. The second equality follows from the fact that the total number of particles, N , is fixed. It is then straightforward to show that the mean and variance are given by $\langle n \rangle = N \cos N\phi$ and $(\Delta n)^2 = \langle n^2 \rangle - \langle n \rangle^2 = (N \sin N\phi)^2$. The phase resolution of this scheme is,

$$(\Delta\phi)^2 = \frac{(\Delta n)^2}{(\partial\langle n \rangle / \partial\phi)^2} = \frac{1}{N^2}. \quad (25)$$

This is the result that we want, and shows that the quantum interferometer allows us to achieve the Heisenberg limit for the phase resolution. This is the same resolution afforded by using cat states directly, as discussed in section 2. However, the true advantage of the quantum interferometer scheme is that it overcomes the problem of detector inefficiencies as we shall now show.

According to the model of nonideal photodetection, the detected field mode $i \in \{3, 4\}$ is described by a photon annihilation operator,

$$a'_i = \sqrt{\mu} a_i + \sqrt{1 - \mu} v_i, \quad (26)$$

where v_i is the annihilation operator for the vacuum state mode [29, 30] and $0 \leq \mu \leq 1$ is the efficiency of the detector. For simplicity, we have taken μ to be the same for both detectors. This is equivalent to considering two perfectly efficient detectors and a beam splitter with transmission coefficient μ in front of each of them. The beam splitters coherently remove a fraction $(1 - \mu)$ of the particles, leaving the fraction μ to be detected.

The number operator for the detected photons at each output port is given by $n'_i = a'_i^\dagger a'_i$ and the signal is $n' = n'_4 - n'_3$. This allows us to obtain the relations,

$$\langle n' \rangle = \mu \langle n \rangle = \mu N - 2\langle n'_3 \rangle \quad (27)$$

$$(\Delta n')^2 = \mu^2 (\Delta n)^2 + \mu(1 - \mu)N. \quad (28)$$

Substituting in the values for $\langle n \rangle$ and $(\Delta n)^2$ that we found above, gives $\langle n' \rangle = \mu N \cos N\phi$ and $(\Delta n')^2 = (\mu N \sin N\phi)^2 + \mu(1 - \mu)N$. Using these relations, the phase uncertainty is given by

$$(\Delta\phi)^2 = \frac{(\Delta n')^2}{(\partial\langle n' \rangle / \partial\phi)^2} = \frac{1}{N^2} + \left(\frac{1 - \mu}{\mu}\right) \frac{1}{N^3 \sin^2 N\phi}. \quad (29)$$

The first term on the right hand side, which is independent of the detector efficiency, represents the ideal case. The second term accounts for detector imperfections and hence vanishes for perfect detectors, $\mu = 1$. The key point is that this second term scales as $1/N^3$, for values of $N\phi$ not too close to integer multiples of π . This means that the destructive effects of realistic detectors are negligible for NOON states with large N .

We can get a better understanding of the restrictions on the values that $N\phi$ can take by linearizing $\sin^2 N\phi$ around $N\phi = 0$ in (29). This shows that, for large N , the first term dominates so long as $\phi > 1/N^{3/2}$. This is a restriction we can happily accept since the smallest phase that we can distinguish from zero scales as $\phi \sim 1/N$. In other words, the effects of detector inefficiencies are unimportant for all relevant cases. This is a remarkable result as detector efficiencies are a major obstacle to beating the standard quantum limit in other precision measurement schemes.

We have shown in this section how the measurement scheme is robust to imperfections in the detectors. In the next section, we shall consider the effects of imperfect quantum beam splitters and shall focus, in particular, on how loss affects our results.

5. Effects of loss

It is well known that macroscopic superposition states, such as the NOON state we have been considering, are highly fragile. In the presence of dissipation, such superpositions are destroyed on timescales corresponding to the loss of a single particle. For this reason, any practical implementation of the measurement scheme outlined above must pay special attention to carefully isolating the NOON state from its environment. It is important that the phase shift, ϕ , is applied to the NOON state on a timescale shorter than that corresponding to the loss of a particle.

In this section, we shall consider a related question. Rather than considering loss on the NOON state itself, we shall investigate the effects of loss during its creation process. Another way of thinking of this is that the quantum beam splitters in our scheme are imperfect or lossy. Such a consideration is clearly important with regard to practical implementations of this scheme.

In figure 5, we have divided the quantum interferometer into three distinct regions (labelled I, II, and III) where loss can occur. We shall see that region II corresponds to dissipation acting on the NOON state and, as discussed above, we will ignore this region in the present discussion. The two remaining regions (I and III) are essentially the same and consist of a nonlinearity and an ordinary 50:50 beam splitter. We shall consider the effects of loss in these two regions together.

The first helpful observation is to recognize that, on the ensemble average, loss and the 50:50 beam splitter operation commute. This means that it makes no difference whether the loss is before or after the beam splitter. Therefore, any loss in region I (for example) up to (but not including) the nonlinearity is equivalent to loss only before the first beam splitter. Following the same argument, loss anywhere in region II is equivalent to loss on the NOON state that exists between the two central

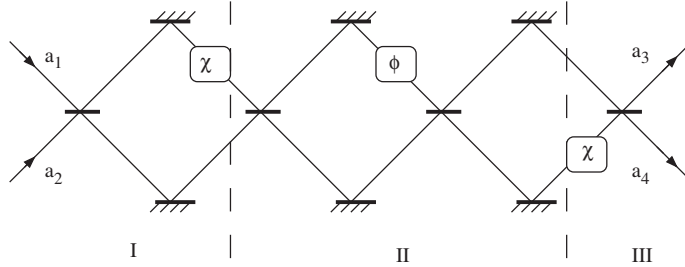


Figure 5. The quantum interferometer with different regions marked I, II, III. We consider how loss of particles in regions I and III affects the precision measurement scheme.

beam splitters. Let us now consider why loss and the beam splitter operation commute.

If the state of a system at time t is given by the density matrix $\rho(t)$, the evolved state under the influence of dissipation is given by the master equation,

$$\dot{\rho}(t) = \Gamma \left[2a_1\rho(t)a_1^\dagger - a_1^\dagger a_1\rho(t) - \rho(t)a_1^\dagger a_1 + 2a_2\rho(t)a_2^\dagger - a_2^\dagger a_2\rho(t) - \rho(t)a_2^\dagger a_2 \right] \quad (30)$$

where we have taken the rate of dissipation, Γ , to be the same in both modes. The operator, U , corresponding to a 50:50 beam splitter is given by (13).

To check that these two operation commute, we need to show that $U\dot{\rho}(t)U^\dagger = d/dt(U\rho(t)U^\dagger)$, i.e. the master equation (and therefore the evolution of the state) is the same whether the loss comes before or after the beam splitter. This can be checked term by term. For example, if we use $UU^\dagger = 1$, we get,

$$\begin{aligned} a_1 U \rho U^\dagger a_1^\dagger + a_2 U \rho U^\dagger a_2^\dagger &= U(U^\dagger a_1 U)\rho(U^\dagger a_1^\dagger U)U^\dagger + U(U^\dagger a_2 U)\rho(U^\dagger a_2^\dagger U)U^\dagger \\ &= \frac{1}{2} U \left[(a_1 + ia_2)\rho(a_1^\dagger - ia_2^\dagger) + (ia_1 + a_2)\rho(-ia_1^\dagger + a_2^\dagger) \right] U^\dagger \\ &= U \left[a_1 \rho a_1^\dagger + a_2 \rho a_2^\dagger \right] U^\dagger, \end{aligned} \quad (31)$$

as required. A similar result holds for the remaining terms of (30) and demonstrates that the processes of equal dissipation in each mode and a 50:50 beam splitter commute.

Referring to figure 5, we see that this result means that any loss in region III (apart from the nonlinearity) is equivalent to loss at the output of the quantum interferometer. We have already shown in section 4 that loss at the output (e.g. by inefficient detectors) does not adversely affect the performance of our scheme. Similarly, any loss in region I (apart from the nonlinearity) is equivalent to loss in the input state. Since we start with a state of the form $|\psi\rangle = |N, 0\rangle$, the loss simply changes the value of N and does not otherwise affect the performance of our scheme.

This is a useful result: it means that, to account for any loss in regions I and III, we only need to consider loss during the nonlinear evolution. We now consider how this affects our results. For simplicity we will consider loss only during the nonlinear

evolution of region III, however, similar results should apply when there is loss in both nonlinearities.

Let us consider that an atom is lost at time ft , where $0 \leq f \leq 1$ is the fraction of the total nonlinear interaction time, t , at which the loss occurred. The state at the end of the interaction time can be shown to be [28],

$$|\psi\rangle = \frac{1}{\sqrt{2^{\tilde{N}}}} \sum_{k=0}^{\tilde{N}} \binom{\tilde{N}}{k}^{1/2} e^{-i\pi[k(k-1)]/2} e^{-i\pi fk} |k\rangle |\tilde{N}-k\rangle, \quad (32)$$

where $\tilde{N} = N - 1$. We notice that this loss introduces a phase factor that shifts the relative phases of the modes by $f\pi$. For multiple losses, the effect is to simply introduce a phase shift of the same general form as that shown in (32). In other words, many losses can be treated in the same way as a single loss.

The effect of loss during the nonlinear evolution has been studied in detail elsewhere [28]. In particular, it has been shown that the phase shift, introduced by loss, degrades the quality of the NOON state at the output. For a flat distribution of random phases introduced by the loss, a simple simulation shows that about 80% of trials give rise to states that look ‘cat-like’. This suggests that we may be able to achieve enhanced measurement resolution in these cases. Indeed, for small phase shifts, it should be possible to recover the Heisenberg limit as we shall now demonstrate.

In figure 6, we have plotted the probability distribution for particles in output mode 3 for a state that has acquired a phase shift of 0.1π due to losses in the nonlinearity of region III, i.e. $f=0.1$ in equation (32). We see that it is a good approximation to a NOON state, but somewhat degraded by the loss, as discussed above.

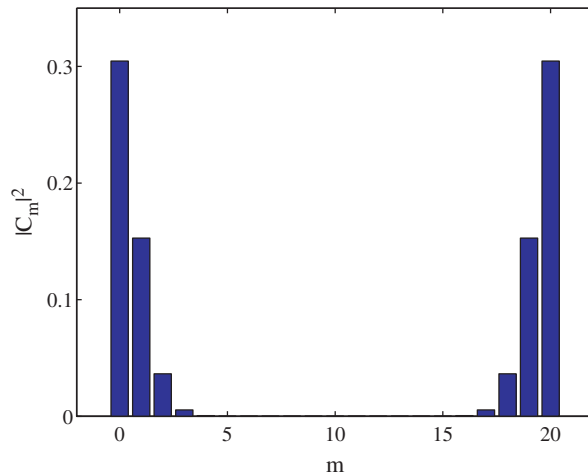


Figure 6. Plot of the coefficients $|C_m|^2$ of (33) for a state that has acquired a phase shift of 0.1π due to losses in the nonlinearity of region III in figure 5. This plot represents the probability distribution of particles in each of the output ports. (The colour version of this figure is included in the online version of the journal.)

We can write the general form of this state by a simple modification of the output state for no loss (22),

$$|\psi\rangle = \frac{i}{2} \sum_{m=0}^{N/2} C_m [(-1)^N (\mathrm{e}^{iN\theta} - 1) |N-m, m\rangle + i^{N-1} (\mathrm{e}^{iN\theta} + 1) |m, N-m\rangle], \quad (33)$$

where $\sum_m |C_m|^2 = 1$. If, as before, we measure $n = n_4 - n_3$ as the signal, a straightforward calculation gives,

$$\langle n \rangle = (N - 2\bar{m}) \cos N\phi \quad (34)$$

$$(\Delta n)^2 = (N - 2\bar{m})^2 \sin^2 N\phi + 4(\Delta m)^2, \quad (35)$$

where $(\Delta m)^2 \equiv \bar{m}^2 - \bar{m}^2$, $\bar{m} \equiv \sum_m |C_m|^2 m$ and $\bar{m}^2 \equiv \sum_m |C_m|^2 m^2$. The square of the phase uncertainty is then given by,

$$(\Delta\theta)^2 = \frac{1}{N^2} + \frac{4(\Delta m)^2}{[N(N - 2\bar{m}) \sin N\phi]^2}. \quad (36)$$

In the case that the disturbance to the NOON state is small, i.e. $\bar{m} \ll N/2$ and $m^2 \ll N^2/4$, which is valid for the state shown in figure 6, equation (36) can be simplified to,

$$(\Delta\phi)^2 \approx \frac{1}{N^2} + \frac{4(\Delta m)^2}{N^4 \sin^2 N\phi}. \quad (37)$$

This reduces to $(\Delta\phi)^2 \approx 1/N^2$ so long as $N\phi$ is not too close to an integer multiple of π . This is a promising result since it means that we can still expect to approach the Heisenberg limit even if there are small imperfections in the quantum beam splitter.

Finally, we would like to consider the full result and investigate the effect on the phase sensitivity of our scheme when we include both imperfect detectors and an imperfect quantum beam splitter. Following a similar calculation to the above one, we obtain,

$$\langle n' \rangle = \mu(N - 2\bar{m}) \cos N\phi \quad (38)$$

$$(\Delta n')^2 = \mu^2(N - 2\bar{m})^2 \sin^2 N\phi + 4\mu^2(\Delta n)^2 + \mu(1 - \mu)N. \quad (39)$$

This gives the phase uncertainty as,

$$(\Delta\phi)^2 = \frac{1}{N^2} + \frac{1}{N(N - 2\bar{m})^2 \sin^2 N\phi} \left[\frac{4(\Delta m)^2}{N} + \frac{1 - \mu}{\mu} \right]. \quad (40)$$

In the limit that $\bar{m} \rightarrow 0$ and $\bar{m}^2 \rightarrow 0$, this reduces to (29) as it should. If we consider the same case as before, i.e. $\bar{m} \ll N/2$ and $m^2 \ll N^2/4$, and $N\phi$ is not too close to an integer multiple of π , then (40) is dominated by the first term. This means that we can once again achieve a resolution in the measurement of the phase shift that scales as $\Delta\phi \sim 1/N$ even if both the quantum beam splitter and the detectors are inefficient. Similar results hold when both beam splitters are imperfect. This is because, if the first quantum beam splitter is slightly imperfect, the state inside the interferometer is very close to a NOON state and should allow measurements

resolutions close to the Heisenberg limit. Since the output beam splitter only marginally degrades the signal, it should still be possible to obtain enhanced measurement resolution when both beam splitters are imperfect. So, while it would be preferable to eliminate losses during the nonlinear evolution, they do not completely destroy the scheme. This ability to tolerate some loss in the cat creation process may be of key importance for practical realizations of this scheme.

6. Conclusion

We have presented a detailed scheme for implementing quantum beam splitters with a simple combination of ordinary 50:50 beam splitters and nonlinearities. By combining two quantum beam splitters into a quantum interferometer, we have shown how it is possible to measure phase shifts with a resolution approaching the Heisenberg limit. The true value of this scheme is that it is remarkably robust to effects that are likely to be important in experiments and have been major stumbling blocks in other similar proposals. In particular, we have shown that quantum interferometers overcome the major problem of detector inefficiencies and can also tolerate some degree of dissipation. While further work would undoubtedly be valuable for understanding fully the practical limitations of this scheme, it is clear that the robustness of quantum interferometers makes them favourable candidates for a practical implementation of entanglement-enhanced measurements. Experiments have already successfully created NOON states in the laboratory and should be able to be scaled up to larger numbers of particles. This suggests that quantum interferometry schemes will be feasible in upcoming experiments and may well provide a valuable route to achieving precision measurements beyond the shot-noise limit.

Acknowledgments

This work was supported by the UK Engineering and Physical Sciences Research Council (Grant No. GR/S99297/01) and the Korea Research Foundation (Grant No. KRF-2002-070-C00029).

References

- [1] D.R. Robinson, *Commun. Math. Phys.* **1** 159 (1965).
- [2] D. Stoler, *Phys. Rev. D* **1** 3217 (1970).
- [3] E.Y.C. Lu, *Lett. Nuovo Cimento* **2** 1241 (1971).
- [4] H.P. Yuen, *Phys. Rev. A* **13** 2226 (1976).
- [5] D.F. Walls, *Nature* **306** 141 (1983).
- [6] C.M. Caves, *Phys. Rev. Lett.* **45** 75 (1980); *Phys. Rev. D* **23** 1693 (1981).
- [7] V. Giovannetti, S. Lloyd and L. Maccone, *Science* **306** 1330 (2004).
- [8] M.J. Holland and K. Burnett, *Phys. Rev. Lett.* **71** 1355 (1993).

- [9] T. Kim, O. Pfister, M.J. Holland, *et al.*, Phys. Rev. A **57** 4004 (1998); T. Kim, J. Shin, Y. Ha, *et al.*, Opt. Comm. **156** 37 (1998).
- [10] S. Feng and O. Pfister, Phys. Rev. Lett. **92** 203601 (2004).
- [11] T. Kim, Y. Ha, J. Shin, *et al.*, Phys. Rev. A **60** 708 (1999).
- [12] R.C. Pooser and O. Pfister, Phys. Rev. A **69** 043616 (2004).
- [13] J.A. Dunningham, K. Burnett and S.M. Barnett, Phys. Rev. Lett. **89** 150401 (2002).
- [14] J.A. Dunningham and K. Burnett, Phys. Rev. A **70** 033601 (2004).
- [15] T. Kim, J.A. Dunningham and K. Burnett, unpublished (2005).
- [16] P. Kok, A.N. Boto, D.S. Abrams, *et al.*, Phys. Rev. A **63** 063407 (2001).
- [17] J.J. Bollinger, W.M. Itano, D.J. Wineland, *et al.*, Phys. Rev. A **54** R4649 (1996).
- [18] R.A. Campos, C.C. Gerry and A. Benmoussa, Phys. Rev. A **68** 023810 (2003).
- [19] J.A. Dunningham, A.V. Rau and K. Burnett, Science **307** 872 (2005).
- [20] X.-B. Zou, J. Kim and H.-W. Lee, Phys. Rev. A **63** 065801 (2001); C.C. Gerry and R.A. Campos, Phys. Rev. A **64** 063814 (2001).
- [21] C.C. Gerry, Phys. Rev. A **61** 043811 (2000).
- [22] H. Lee, P. Kok, N.J. Cerf, *et al.*, Phys. Rev. A **65** 030101 (2002).
- [23] P. Kok, H. Lee and J.P. Dowling, Phys. Rev. A **65** 052104 (2002).
- [24] J. Jacobson, G. Björk, I. Chuang, *et al.*, Phys. Rev. Lett. **74** 4835 (1995).
- [25] K. Mølmer and A. Sørensen, Phys. Rev. Lett. **82** 1835 (1999).
- [26] M.W. Mitchell, J.S. Lundeen and A.M. Steinberg, Nature **429** 161 (2004).
- [27] C.A. Sackett, D. Kielpinski, B.E. King, *et al.*, Nature **404** 256 (2000).
- [28] J.A. Dunningham and K. Burnett, J. Mod. Opt. **48** 1837 (2001).
- [29] H.P. Yuen and J.H. Shapiro, IEEE Trans. Inf. Theory IT**26** 78 (1980); *Coherence and Quantum Optics IV*, edited by L. Mandel and E. Wolf (Cambridge University Press, Cambridge, 1978), p. 719.
- [30] B. Yurke, Phys. Rev. A **32** 311 (1985).